Analytica Chimica Acta 751 (2012) 161–170

Contents lists available at SciVerse ScienceDirect

Analytica Chimica Acta

journal homepage: www.elsevier.com/locate/aca

Towards an integrated biosensor array for simultaneous and rapid multi-analysis of endocrine disrupting chemicals

Viviana Scognamiglio[a,*], Italo Pezzotti[b], Gianni Pezzotti[b], Juan Cano[b], Ivano Manfredonia[b], Katia Buonasera[a], Fabiana Arduini[c], Danila Moscone[c], Giuseppe Palleschi[c], Maria Teresa Giardi[a]

[a] IC-CNR Istituto di Cristallografia, AdR1 Dipartimento Agroalimentare – Via Salaria Km 29.3 00015, Rome, Italy
[b] Biosensor S.r.l. – Via degli Olmetti 44 00060 Formello, Rome, Italy
[c] Università di Roma Tor Vergata, Dipartimento di Scienze e Tecnologie Chimiche – Via della Ricerca Scientifica 00133, Rome, Italy

HIGHLIGHTS

- A multitask biosensor for the detection of endocrine disrupting chemicals is proposed.
- The sensing system employ an array of biological recognition elements.
- Amperometric and optical transduction methods are provided in an integrated biosensor together with flow control systems.
- The biosensing device results in an integrated, automatic and portable system for environmental and agri-food application.

GRAPHICAL ABSTRACT

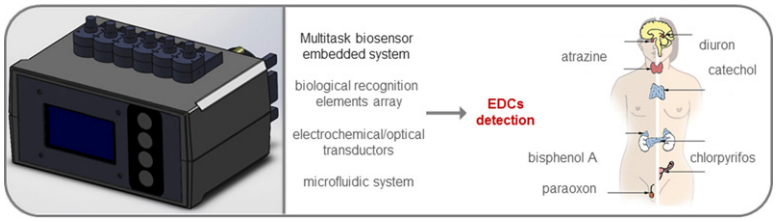

ARTICLE INFO

Article history:
Received 23 April 2012
Received in revised form 6 September 2012
Accepted 7 September 2012
Available online 18 September 2012

Keywords:
Endocrine disrupting chemicals
Multi-array
Biosensor
Amperometric
Optical
Integrated biosensing system

ABSTRACT

In this paper we propose the construction and application of a portable multi-purpose biosensor array for the simultaneous detection of a wide range of endocrine disruptor chemicals (EDCs), based on the recognition operated by various enzymes and microorganisms. The developed biosensor combines both electrochemical and optical transduction systems, in order to increase the number of chemical species which can be monitored. Considering to the maximum residue level (MRL) of contaminants established by the European Commission, the biosensor system was able to detect most of the chemicals analysed with very high sensitivity. In particular, atrazine and diuron were detected with a limit of detection of 0.5 nM, with an RSD% less than 5%; paraoxon and chlorpyrifos were revealed with a detection of 5 μM and 4.5 μM, respectively, with an RSD% less than 6%; catechol and bisphenol A were identified with a limit of detection of 1 μM and 35 μM respectively, with an RSD% less than 5%.

1. Introduction

Over the past 50 years, thousands of chemicals have been synthesized and released into the environment, resulting in the contamination of food, plants and animals. Because of their structural similarity with endogenous hormones and ability to interact with hormone transport proteins, these chemicals have the potential to influence the endocrine system, altering its normal action. These substances, being able to interfere with the synthesis, secretion, transport, binding, action or elimination of natural hormones, have been described as endocrine disrupting chemicals (EDCs) [1–4].

* Corresponding author.
E-mail address: viviana.scognamiglio@mlib.ic.cnr.it (V. Scognamiglio).

0003-2670/$ – see front matter © 2012 Elsevier B.V. All rights reserved.
http://dx.doi.org/10.1016/j.aca.2012.09.010

EDCs include different classes of compounds, such as, surfactants, plasticizers, organohalogens, pharmaceuticals, natural hormones and several others. Among these, pesticides represent the portion of chemical species with the highest environmental impact. Several pesticides in agriculture, or employed at home and urban areas, have been identified as potential endocrine disruptors: e.g. atrazine, dicofol, methylbromide, carbendazim, prochloraz, dibromoethane, diuron, diazinon, propanil, paraoxon, chlorpyrifos and several others [1–4].

EDCs can affect the endocrine system through different mechanisms of action, for example: by binding oestrogen receptors, causing activation or inactivation; modifying the metabolism of natural hormones or the number of hormone receptors in a cell; modifying the production of natural hormones interfering in other signalling systems [5–8]. Several effects on human health have been documented, ranging from acute to chronic health effects such as cancers, birth defects, reproductive harm, neurological and developmental toxicity, immunotoxicity [9–11]. Moreover, several impacts on diabetes and obesity have been reported [12,13].

Given the latest statistics on the toxic effect of EDCs on human and wildlife health, various organisations have published lists of suspected endocrine disruptors, with regards to the type of chemicals and the admitted concentration present in the environment. The European Commission Scientific Committee for Toxicity, Ecotoxicity and the Environment (SCTEE) presented in 1999 the report "Human and Wildlife Health Effects of Endocrine Disrupting Chemicals, with emphasis on Wildlife and on Ecotoxicology test methods" (SCTEE 1999), it identified a "potential global problem" for wildlife concerning physiological changes in reproduction and development systems linked to the exposure to EDCs. In December 1999, the European Commission adopted a Communication to the Council and the European Parliament on a Strategy for EDCs management (COM (1999) 706 [14]). In June 2001 the Commission adopted a follow-up Communication on the implementation of the Strategy for EDCs (COM (2001) 262 [15]). Consequently, there is now considerable interest in monitoring their presence in order to safeguard the health of ecosystems. The principal challenge in EDCs detection originates from their chemical heterogeneity. As a consequence of their variety and class specificity, a collection of several analytical methodologies has been developed over the years for the detection of a wide range of chemical species. In this context, techniques such as gas chromatography and high-performance liquid chromatography with UV and/or mass spectrometry detection, represent the most used techniques to monitor the presence of endocrine disruptors. In recent years, the development of new, advanced methodologies for rapid, inexpensive and in field environmental monitoring based on biosensing mechanisms represent a promising research challenge [14–21] and has resulted recently in the publication of a few articles in this area.

In this paper we described the development of an automatic biosensing array which employs several types of biological sensing elements, for the detection of a wide range of chemical species, and combines the most used transducers for biosensor, amperometric and optical systems. The multi-function multi-transduction system can give complementary information about the modification of current signals, correlated to the electrogenic property of the biocomponents, and the modification of fluorescence signals correlated to a conformational or chemical modification. Both of these can be linked to the presence of the target analyte in an analyte concentration dependent manner.

The novelty of this work was to generate a biosensing system employing different biocomponents coupled to two transduction systems and having these integrated in a very smart biosensor configuration for a versatile, reliable and sensitive detection of a wide collection of EDCs.

2. Materials and methods

2.1. Reagents

All chemicals from commercial sources were of analytical grade. Glutaraldehyde (GAD, 25%, v/v, aqueous solution), Nafion® (perfluorinated ion-exchange resin, 5% (v/v) solution in lower alcohols/water), Bovine serum albumin (BSA) were purchased from Sigma (St. Louis, MO). Acetylcholinesterase from *Electric eel* and Butyrylcholinesterase from *horse serum*, Laccase from *Trametes versicolor* and Tyrosinase from Horseradish were supplied by Sigma (St. Louis, MO). Fluorescein 5(6)-isothiocyanate (FITC) and Carboxynaphthofluorescein were from Molecular Probes/Invitrogen. Graphite and Prussian Blue modified graphite screen printed electrodes (SPEs) were purchased from DropSens (Asturias, ES), with a screen printed Ag reference and graphite counter electrode.

2.2. Biosensing system set up

EDCs monitoring was performed by using an array of biological recognition elements able to recognize a wide range of chemical classes. The following sections are devoted to the description of the biocomponents configuration and to the biosensing device development.

2.2.1. Acetylcholinesterase/butyrylcholinesterase

Acetylcholinesterase/butyrylcholinesterase enzyme solutions were prepared by weighting a suitable amount of powder with known enzymatic activity and solubilising it in 0.1 M PBS buffer solution pH 8.0. 2 μl of 1% glutaraldehyde in water was dropped on a Prussian Blue modified screen printed electrode (SPE) and left at 4 °C until the suspension had dried. Then, 2 μl of a mixture of BSA, enzyme and Nafion® were spotted by drop-casting on the working electrode of each SPE. The mixture was obtained by mixing 25 μl of BSA (5% (w/v) prepared in water), 25 μl of Nafion® (1% (v/v) diluted in water) and 25 μl of an enzyme stock. The electrodes were left at 4 °C in a dry chamber with $CaCl_2$ until the enzyme suspension was dry.

Amperometric measurements were carried out at room temperature in 0.1 M KCl, 0.1 M PBS pH 8.0. The amperometric parameters used for the procedure were chosen on the basis of the voltammetric analysis conducted on the specific substrate that was recognised and hydrolysed by the enzyme. Pump flow was set at 200 μl/min, potential at +200 mV vs Ag pseudoreference. The procedure for the evaluation of the effect of the enzyme activity inhibition due to the presence of pesticides on the biosensor response included the following steps. The biosensor was loaded into the measurement cell and 0.1 M KCl + 0.1 M PBS, pH 8.0 was flowed in by the peristaltic pump until a stable baseline output signal was reached. A solution of 5 mM of Butyrylthiocholine in 0.1 M KCl + 0.1 M PBS, pH 8.0 was flowed in and the current variation was recorded. This current signal represented the biosensor response and was used for further evaluation of the inhibition effect in order to determine the pesticide concentrations. Then, solutions of the analysed pesticide, in a range between 10 and 150 μM in 0.1 M KCl + 0.1 M PBS, pH 8.0, were flowed and incubated for 10 min. A solution of 5 mM of Butyrylthiocholine in 0.1 M KCl, 0.1 M PBS pH 8.0 was flowed again and the current variation was recorded. The detection of the organophosphorous and organothiophosphorous pesticides is simply based on the determination of the difference in enzyme activity in the presence and absence of inhibitor, according to the following the Eq. (1):

$$I\% = \left[\frac{(A_0 - A_i)}{A_0}\right] \times 100 \quad (1)$$

where A_0 is the activity in absence of inhibitor, and A_i in presence of inhibitor.

Optical measurements were carried out at room temperature in 2 mM PBS pH 8.0. The measurements were carried out in static mode by incubation of Acetylcholinesterase enzyme with the analysed pesticide in the presence of a pH-sensitive dye. The optical parameters used for the procedure were chosen on the basis of the fluorescence properties of the pH-sensitive fluorescent probe. Since the Carboxynaphthofluorescein showed an absorption maximum peak at 598 nm and a fluorescence emission maximum peak at 668 nm, the instrument was set to show these values of wavelength for the excitation and the emission of the probe.

The procedure for the evaluation of the effect of the inhibition of enzyme activity due to the presence of pesticides on the biosensor response included the following steps. A solution of 13U Acetylcholinesterase was added to the measurement cell containing Carboxynaphthofluorescein with a concentration of 1.5 μM. The optical signal was recorded and correlated to the fluorescence value typical of a solution at pH 8.0. Then, a solution of 5 mM of Acetylthiocholine in 2 mM PBS pH 8.0 was added and incubated for 1 min, in order to register the optical signal related to the biosensor response. At this point, samples containing different amounts of pesticide were incubated in solutions of 13U Acetylcholinesterase for 30 min and the biosensor responses were evaluated by adding 5 mM of Acetylthiocholine in 2 mM PBS pH 8.0. The inhibition rate was determined by comparing the response of the biosensor before and after exposure to the pesticide solutions. Fluorescence intensity values were plotted as a function of the increasing concentration of pesticide to obtain a calibration curve.

2.2.2. Tyrosinase

A Tyrosinase enzyme solution was prepared by weighting a suitable amount of powder with known enzymatic activity and solubilising it in 0.1 M PBS buffer solution pH 6.5. Aliquots of 5 μl of Tyrosinase enzyme solution were taken and spotted by drop-casting on a graphite screen printed electrode. Each electrode was left in a dry chamber with $CaCl_2$ at 4 °C until the enzyme suspension resulted dry. 5 μl of a Nafion® 1% solution in 0.1 M PBS buffer solution pH 6.5 was dropped on the dried enzyme suspension and left again at 4 °C until suspension resulted dry.

For enzyme labelling, a threefold excess of Fluorescein 5(6)-isothiocyanate (FITC) in dimetyl formamide was added drop-wise to a solution of 5.0 mg/ml of tyrosinase or laccase enzymes in 0.1 M Sodium Bicarbonate pH 9.0, and then the solution was left to react for 1 h at 37 °C protected from light. The resulting labelled enzymes were separated from the free dye by Sephadex G-25 column. Measurements of absorption between 220 and 600 nm of each fraction were achieved to detect the conjugates. The eluted fractions, corresponding to the first fluorescent volume excluded, represented the labelled enzymes. The fractions containing the conjugates were pooled and a final absorbance spectrum was recorded to determine the degree of labelling. The relative efficiency of the labelling reaction was determined by measuring the absorbance of the enzymes at 280 nm and the absorbance of the dyes at its absorbance maximum. Using the Beer–Lambert law the approximate number of dye molecules per protein molecule was calculated. Initially the protein concentration was determined and corrected for the contribution of the dye to the absorbance at A_{280} according to the Eq. (2):

$$\text{Correction factor(CF)} = \frac{A_{280}\text{free dye}}{A_{\max}\text{free dye}} \quad (2)$$

$$A_{\text{enzyme}} = A_{280} - (A_{280} \times CF) \quad (3)$$

The protein concentration was calculated and the degree of labelling (DOL) was determined according to the Eq. (4):

$$\text{DOL} = \frac{(A_{\max} \times \text{MW})}{([\text{enzyme}] \times E_{\text{dye}})} \quad (4)$$

in which $A_{\max}$ is the maximum absorbance of dyes, MW is the molecular weight, E_{dye} is the extinction coefficient of the dyes at their absorbance maximum and the protein concentration is in mg ml^{-1}.

Amperometric measurements were carried out at room temperature in 0.1 M PBS pH 6.5. The amperometric parameters used for the procedure were chosen on the basis of the voltammetric analysis conducted on catechol when it was recognised and oxidised by the Tyrosinase. Pump flow was set at 200 μl/min, potential at −200 mV vs Ag pseudoreference. Determination of catechol was carried out electrochemically by measuring the intensity of current, which corresponds to the electrochemical reduction of the generated quinone.

The procedure for the evaluation of the presence of catechol included the following steps. The Tyrosinase biosensor was loaded in the measurement cell and 0.1 M PBS pH 6.5 was flowed by the peristaltic pump until a stable baseline output signal was reached. Then, solutions at different concentrations of catechol in 0.1 M PBS pH 6.5 were flowed and the current variation was recorded. The biosensor response was evaluated by a one-shot measurement due to the low cost of the sensor used, showing a high intra and inter-electrode repeatability ($n = 5$) for each concentration tested in the linear range of response.

The current signals represented the biosensor response and were related to the different catechol concentrations plotted to obtain a calibration curve.

Optical measurements were carried out at room temperature in 0.1 M PBS pH 6.5. The optical parameters used for the procedure were chosen on the basis of the fluorescence properties of the fluorescent probe used for the Tyrosinase enzyme labelling. Since FITC showed an absorption maximum peak at 492 nm and a fluorescence emission maximum peak at 518 m, the instrument was set to show these values of wavelength for the excitation and the emission of the probe. The FITC-labelled Tyrosinase was immobilized on the surface of the SPE and the same procedure for the amperometric evaluation of the presence of catechol was followed.

2.2.3. Laccase

Laccase enzyme was utilized as biological recognition element for phenolic compounds. A Laccase enzyme solution was prepared by weighing a suitable amount of powder with known enzymatic activity and solubilising it in 0.1 M PBS buffer solution pH 4.5. Aliquots of 5 μl of Laccase enzyme solution were taken and spotted by drop-casting on graphite SPEs. The electrodes were left in a dry chamber with $CaCl_2$ at 4 °C until the enzyme suspension resulted dry. 5 μl of a Nafion® 1% solution in 0.1 M PBS buffer solution pH 4.5 was dropped on the dried enzyme suspension and left again at 4 °C until the suspension was dry.

Amperometric measurements were carried out at room temperature in 0.1 M PBS pH 4.5. The amperometric parameters used for the procedure were chosen on the basis of the voltammetric analysis conducted on bisphenol A recognised by the laccase. Pump flow was set at 200 μl/min, potential at −30 mV vs Ag pseudoreference. Determination of bisphenol A was carried out electrochemically by measuring the intensity of current, which corresponds to the electrochemical reduction of the generated quinone. The laccase biosensor was loaded in the measurement cell and 0.1 M PBS pH 4.5 was flowed by the peristaltic pump until a stable baseline output signal was reached. Solutions of different concentrations of bisphenol A in 0.1 M PBS pH 4.5 were flowed and the current variation was recorded. The biosensor response

was evaluated by a one-shot measurement due to the low cost of the sensor used. However, the biosensor employed showed high repeatability for both intra and inter-electrode measurements ($n = 5$).

2.2.4. Photosystem II

Whole cells of different genetic variants [16,22] of the green photosynthetic algae *C. reinhardtii* were collected in order to obtain a final concentration of 7/8 O.D. corresponding to 2.25×10^5 cells immobilized on each electrode. The activity of algae cells suspension was verified by measuring chlorophyll fluorescence in terms of F_V/F_M activity (Fluorescence Monitoring System, Hansatech Instruments Ltd., UK). The algae suspension at 7/8 O.D. was centrifuged at $14{,}560 \times g$ for 2 min. The supernatant was discarded and the pellet re-suspended twice in a medium containing 20 mM Tricine, 70 mM Sucrose, 5 mM $MgCl_2$, 50 mM NaCl pH 7.2. The final supernatant was discarded and the pellet re-suspended in the same medium to have a total suspension of 50 μl. Aliquots of 5 μl of *C. reinhardtii* concentrated suspension were taken and spotted by drop-casting on graphite SPEs. The electrodes were left at 4 °C in a dry chamber with $CaCl_2$ until the algae suspension resulted dry. 5 μl of a Nafion® 1% solution in 20 mM Tricine, 70 mM Sucrose, 5 mM $MgCl_2$, 50 mM NaCl pH 7.2 buffer was dropped on the dried algae suspension and left again at 4 °C until suspension was dry.

Optical measurements were carried out at room temperature in 20 mM Tricine, 70 mM Sucrose, 5 mM $MgCl_2$, 50 mM NaCl pH 7.2 buffer. Pump flow was set at 200 μl/min. Determination of pesticides was carried out optically by measuring the fluorescence parameters (basal fluorescence F_0, fluorescence at 2 ms F_J, fluorescence at 200 ms F_I, maximum fluorescence F_M) and the relative variable fluorescence $V_J = (F_J - F_0)/(F_M - F_0)$ of the Kautsky fluorescence transient curve in the absence and in the presence of the target analytes. The optical parameters used for the procedure were chosen on the basis of the fluorescence properties of the photosynthetic microorganism. Since *C. reinhardtii* showed an absorption maximum peak at 660 nm and a fluorescence emission maximum peak at 690 nm, the instrument was set to these values of wavelength for the excitation and emission of the biological material. The immobilised SPEs were loaded in the measurement cell and 20 mM Tricine, 70 mM Sucrose, 5 mM $MgCl_2$, 50 mM NaCl, pH 7.2 buffer was flowed by the peristaltic pump. Solutions of different concentration of pesticide in 20 mM tricine, 70 mM Sucrose, 5 mM $MgCl_2$, 50 mM NaCl pH 7.2 buffer were fluxed and the variation of fluorescence parameters was analysed. These optical parameters represented the biosensor response and were related to the different pesticide concentrations plotted to obtain a calibration curve.

For each biocomponent, a real sample solution was flowed and the fluorescence signal was recorded; the resulted fluorescence value was plotted on the calibration curve and the corresponding concentration of contaminant was calculated. Each experiment was repeated three times in order to evaluate the biosensor repeatability.

2.3. Device overview

The miniaturized biosensing array system was designed to be flexible, modular and small, with six independent sensing cells equipped with optical excitation and detection, current measurement and flow control systems. The configuration of the array was designed for a wide number of biological recognition elements. In Fig. 1 a scheme of the assembled prototype of the biosensor array equipped with six cells is shown.

The device was based on an innovative measurement cell made up by two separated independent sensing modules, electrochemical and optical, integrated into a compact miniaturized sensor (external diameter 30 mm, height 40 mm).

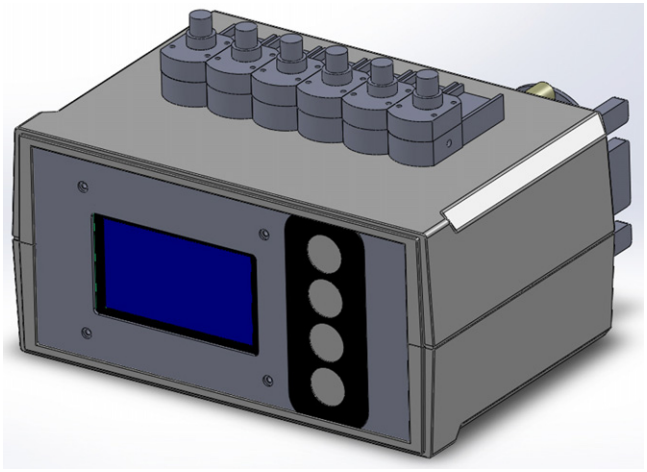

Fig. 1. 3D computer aided design (CAD) view of the biosensor device.

The electrochemical sensing module was composed of the top flow electrochemical cell hosting the biological material, directly deposited on the SPEs, and by inlet and outlet connections for the electrolytic/washing solution and sample flow. The electrochemical set-up was constituted of a DC voltage supply, which provided a bias potential in the range of ±0.625 V between the working and the reference electrodes, and an amperometer to detect the current intensity variation deriving from a biological process. The output current was measured between the working and the counter electrode through two independent recording channels (one per cell) and a data acquisition system, controlled by the central microcontroller unit. The microcontroller was also used to drive the LEDs and the pump and to regulate the light and flow intensity.

The optical module was composed by the bottom static chamber hosting the excitation light sources and by the photodetector coupled to an interferential band-pass filter for fluorescence capture. The optical module provided light excitation in the case of fluorescent biocomponents. A set of LEDs (Ø 3 mm) with the appropriate emission wavelengths were mounted in each optical cell to provide a flexible excitation and fluorescence emission settings for different biological compounds. A high-pass filter was coupled to the silicon photodiode to capture the fluorescence emission spectral range. A glass window separated the optical compartment from the cell hosting the biological material. In Fig. 2 a conceptual cross section of the biosensor cell is shown.

The cells were designed to work with different commercial SPEs and made of an inert material (light acetal resin) featuring low friction and high temperature resistance (max 90 °C). The cell dimension depended on the *o*-ring thickness, resulting in a final volume of 50 μl. Such a small volume makes the flow exchange very fast, thus increasing the response time of the sensor. The electrolytic solution was flown into the cells through three small holes in the glass window in order to protect the biomaterial from leakage and physical damage derived by a strong impact with the buffer flux. The flow was automatically supplied, through tubes of 2 mm diameter, by a double rotary peristaltic pump (40 mm × 50 mm) with adjustable speed (from a minimum value of 200 μl/min up to a maximum of 350 μl/min). The flow cells allowed a dynamic monitoring of the biocomponent reaction with the analyte and, therefore, allowed for an in depth study of their interactions as well as higher measurement accuracy and reliability. The flow rate was chosen to allow the better sensitivity of each biomediator (data not shown). The instrument was suitable also for use in static mode, since the cells were designed to perform measurements in steady

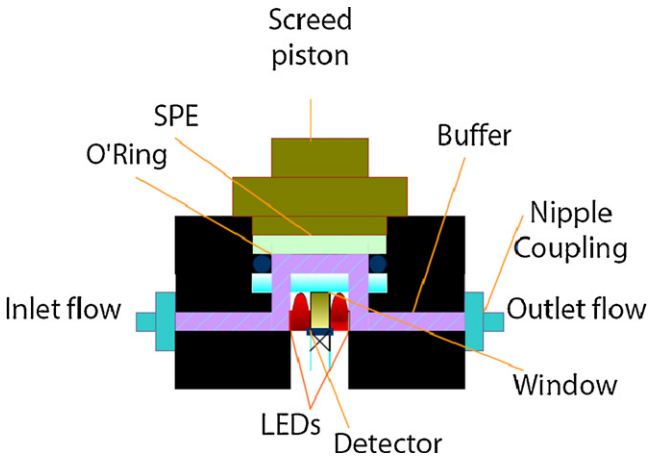

Fig. 2. Conceptual cross section of the biosensor cell equipped with the optical components at the bottom (with two excitation LEDs, central photodiode and filter), SPE biosensor and flow system on top. A piston with a screwed cylinder provided the mechanical support for sealing the biologic compartment by pressing on the *o*-ring.

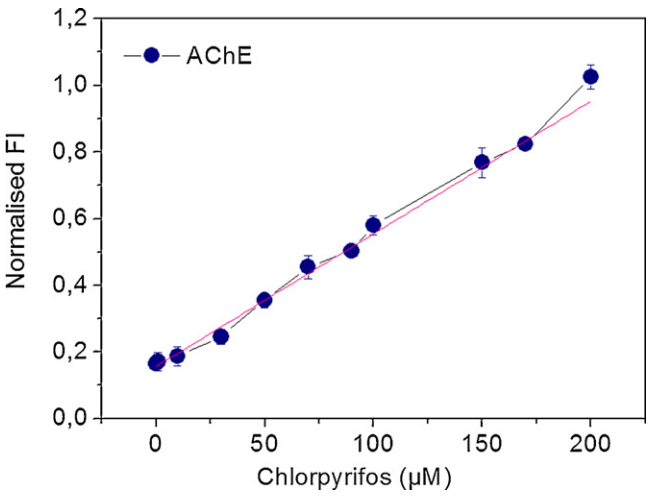

Fig. 3. Calibration curves for chlorpyrifos by optical analysis employing acetylcholinesterase enzyme.

state. The electronic control board mounted inside the instrument included a microcontroller (from Silicon Lab) for the automatic control of the fluidic system (pump, valves), LED drivers, a preprocessing signal conditioning module (amplification and filtering), a timer, a flash memory card for data storage in-field applications. The sensors worked in a continuous and dynamic mode and all detected data were stored and transmitted to the computer by a USB cable connection. Power was supplied internally by lithium batteries or externally for the case of laboratory applications.

3. Results and discussion

We have designed and built a multi-analyte biosensor platform which employs various biological recognition elements and two transduction systems, in order to obtain a biosensing configuration which enables a real-time parallel monitoring of multiple analytes, and allows for a reduction in time, costs and sample volume needed for the measurements. The array of biocomponents was configured as shown in Table 1 and consists of enzymes and microorganisms, capable of detecting the main classes of EDCs. Six classes of chemicals were selected, which are those repeatedly reported in main the above-mentioned European legislations. The performance of the biosensor was studied in order to evaluate the most important analytical parameters of the biosensor, such as limit of detection (LOD), relative standard deviation (RSD%), linear range, response time, reproducibility. In particular, LOD values were calculated as 3 times the standard deviation (S.D.) of the blank/slope ratio, while RSD% values were estimated on 5 repetitive measurements of intra- and inter-electrodes analysis and calculated as the slope.

As presented in Table 1, hydrolytic and oxidase enzymes and photosynthetic organisms were employed to construct an array of biocomponents able to reveal the main EDCs present as environmental and agrifood pollutants; these include organophosphorous and organothiophosphorous pesticides, phenolic compounds and triazinic and ureic herbicides, which are reported in several lists of priority analytes.

Acetylcholinesterase and butyrylcholinesterase enzymes were employed for the detection of organothiophosphorous pesticides, such as chlorpyrifos, or organophosphorous pesticides, such as paraoxon. In particular, an optical biosensing mechanism was developed conjugating the commercial fluorescent probe carboxynaphthofluorescein to the acetylcholinesterase enzyme from *Electric eel*, in order to sense the pH variation of the solution due to the hydrolysis of the acetylthiocholine into choline and acetic acid. In the presence of organothiophosphorous compounds the enzyme activity was inhibited since they covalently block the active site of acetylcholinesterase. This irreversible inactivation leads to an accumulation of acetylcholine and to a different variation of pH value. Consequently, the pH variation led to a fluorescence variation of carboxynaphthofluorescein probe, which can be related to pesticide concentration. In Fig. 3a calibration curve for the detection of chlorpyrifos in the micromolar range is reported. In the presence of different amounts of chlorpyrifos, the acetylcholinesterase biosensor showed a decrease in the current signals, with limit of detection of 7.5 μM and a broad linear range between 0.1 and 200 μM. The regression equation of the linear part of the curve was $y = 0.0039 \pm 7 \times 10^{-5}\ x + 0.1558 \pm 0.007$, where y represents the normalized fluorescence intensity and x the chlorpyrifos concentration in μM; the R^2 was 0.9953. Reproducibility was also calculated and the RSD% was less than 6%. The response time needed to reach 90% of the steady state response was 120 s.

By contrast, an amperometric biosensor mechanism based on butyrylcholinesterase enzyme from *horse serum* was chosen for the detection of organophosphorous pesticides. In particular, the inhibitory effect of paraoxon on butyrylcholinesterase was evaluated by determining the decrease in the current obtained for the oxidation of enzymatic production thiocholine catalysed by the electrochemical mediator Prussian Blue [23]. Butyrylcholinesterase was incubated for 10 min in the pesticide solution, the response toward the substrate was measured and the degree of inhibition was calculated as a relative decay of the biosensor response as reported in Eq. (1) [23]. The reproducibility of the biosensor obtained was quite good as reported in Fig. 4. A RSD% of 3% was observed for five replicates using the Butyrylcholinesterase biosensor, which showed a limit of detection of 12 μM in a linear range between 5 and 150 μM. The regression equation of the linear part of the curve was $y = 0.78 \pm 0.01\ x + 13.75 \pm 1.1$, where y represents the current in % of inhibition and x the paraoxon concentration in μM; the R^2 was 0.99504. The response time needed to reach 90% of the steady state response was 10 s.

The detection of phenolic compounds was performed by using oxidase enzymes such as Tyrosinase and Laccase combined with both electrochemical and optical transduction systems. The enzymes were immobilised on the surface of screen printed electrodes and, in this electrochemical configuration, since the oxidation of phenolics by Tyrosinase brings to quinone compounds, where the released quinone species that are catalytically oxidized by the enzymes were electrochemically reduced and detected in

Table 1
Biological recognition elements selected as array of biocomponents for the detection of EDCs.

Target	Biocomponent	Immobilisation	Technique	Mechanism
Paraoxon	BChE	Cross-linking immobilisation on PB-SPE with BSA/GA/Nafion	Amperometric	Change of current signals owed to competitive inhibition of enzyme by target analyte
Chlorpyrifos	AChE	Cross-linking immobilisation on PB-SPE with BSA/GA/Nafion	Optical	Change of fluorescence emission of CNF due to competitive inhibition of enzyme by target analyte
Catechol	Tyrosinase	Absorbing immobilisation on graphite-SPE with Nafion	Amperometric	Change of current signals owed to oxidation of target analyte
Catechol	FITC-Tyrosinase	Absorbing immobilisation on graphite-SPE with Nafion	Optical	Change of the fluorescence emission of FITC due to binding of target analyte
Bisphenol A	Laccase	Absorbing immobilisation on graphite-SPE with Nafion	Amperometric	Change of current signals owed to oxidation of target analyte
Atrazine Diuron	Algae	Entrapment immobilisation on graphite-SPE with BSA-GA polymer	Optical	Change of fluorescence emission due to inhibition of algae by target analyte

Legend. GA: glutaraldehyde, BSA: bovine serum albumin, AChE: acethylcholinesterase, BChE: butyrylcholinesterase, PB-SPE: Prussian Blue screen printed electrode, CNF: carboxynaphthofluorescein, FITC: fluorescein isothiocyanate.

a concentration-dependent manner. In this context, a Tyrosinase from the common mushroom *Agaricus bisporus* and a fluorescence variant of the enzyme were employed to reveal catechol by both amperometric and fluorescence analysis. In the presence of catechol, the Tyrosinase enzyme showed an increase in the current signals related to the different concentrations of catechol, as shown in Fig. 5, with limit of detection of 25 μM in a linear range between 50 and 400 μM. The regression equation of the linear part of the curve was $y = 0.27 \pm 0.01\,x + 98.96 \pm 2.5$, where y represents the current in nA and x the catechol concentration in μM; the R^2 was 0.9919. Reproducibility was calculated and the RSD% was less than 5%. The response time needed to reach 90% of the steady state response was 10 s.

A fluorescent variant of Tyrosinase enzyme from *A. bisporus* was used for the optical detection of catechol in order to corroborate the amperometric data. In detail, in the presence of catechol, the FITC-labelled Tyrosinase showed a decrease in the fluorescence emission, indicating that the binding of catechol to the enzyme displaced the fluorescence probes into a different environment as a result of a structural conformational change of the protein. In particular, the effect of the fluorescence emission decrease of FITC-labelled Tyrosinase was observed in the presence of micromolar concentrations of catechol, as shown in Fig. 6, with a limit of detection of 10 μM in a linear range between 0.1 and 200 μM. The regression equation of the linear part of the curve was $y = -0.24 \pm 0.009\,x + 57.55 \pm 0.9$, where y represents the fluorescence intensity in arbitrary units (a.u.) and x the catechol concentration in μM; the R^2 was 0.9918. Reproducibility was

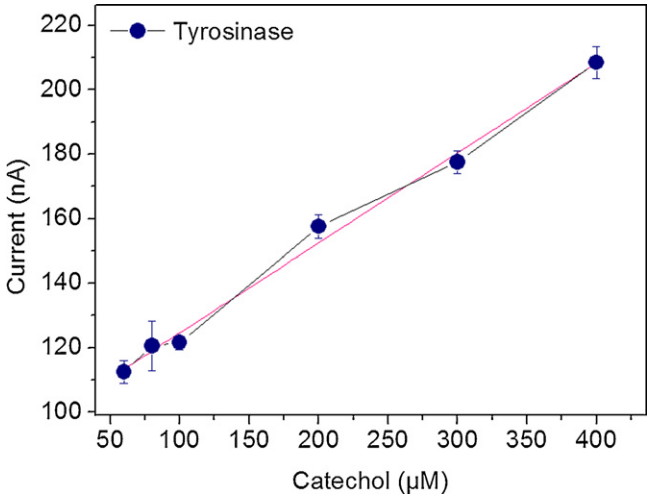

Fig. 5. Calibration curves for catechol by amperometric analysis employing tyrosinase enzyme.

calculated and the RSD% was less than 5%. The response time needed to reach 90% of the steady state response was 30 s.

A Laccase enzyme from the mushroom *Trametes versicolor* was employed for the development of a biosensing system for the detection of bisphenol A, as shown in Fig. 7. Even in this case, the reproducibility of the biosensor was good, showing an RSD% value

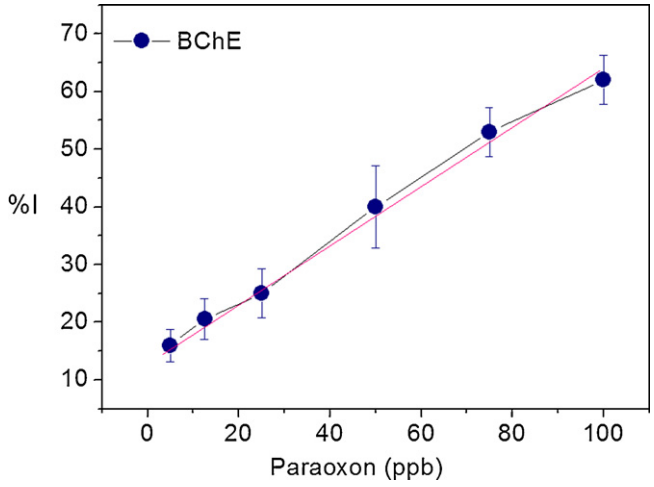

Fig. 4. Calibration curves for paraoxon by amperometric analysis employing butyrylcholinesterase enzyme.

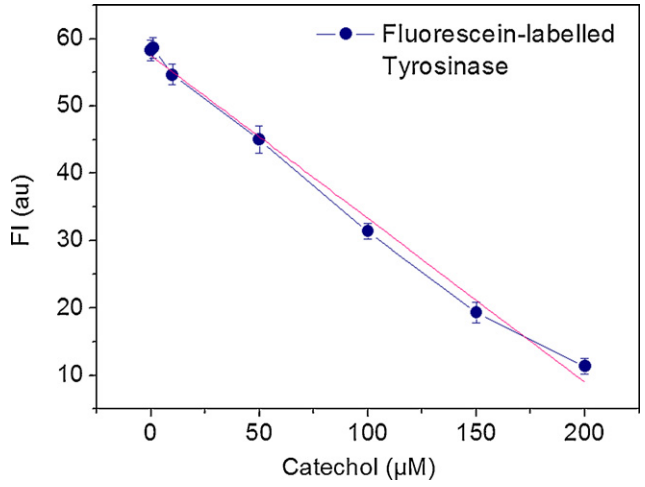

Fig. 6. Calibration curves for catechol by optical analysis employing FITC-labelled tyrosinase enzyme.

Table 2
Scheme of the reaction equations and measurement parameters of the array of biocomponents for the detection of EDCs.

Biosensors and reaction mechanisms

BChE-paraoxon

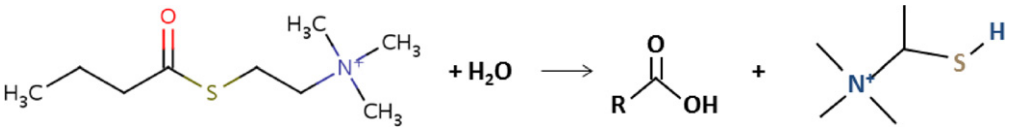

In the presence of paraoxon the enzyme activity is inhibited inducing an accumulation of butyrylthioylcholine and a change in the current signal. The % of inhibition is calculated and related to the target analyte concentration.

AChE-chlorpyrifos

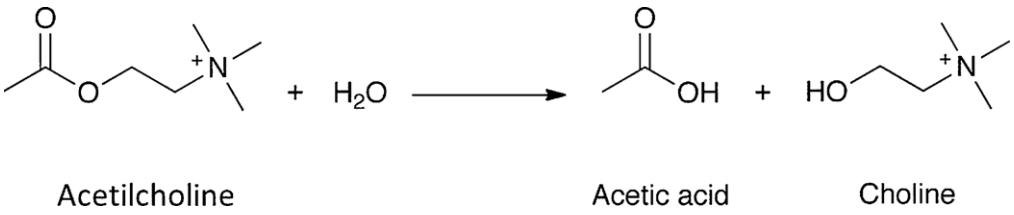

In the presence of chlorpyrifos the enzyme activity is inhibited inducing an accumulation of acetylthiocholine and to a different variation of pH values. CNF is able to sense the pH variation and correlate it to the target analyte concentration.

Tyrosinase-catechol

The enzyme catalyses the oxidation of catechol inducing a variation of current signals, which are related to the target analyte concentration.

FITC/Tyrosinase-catechol

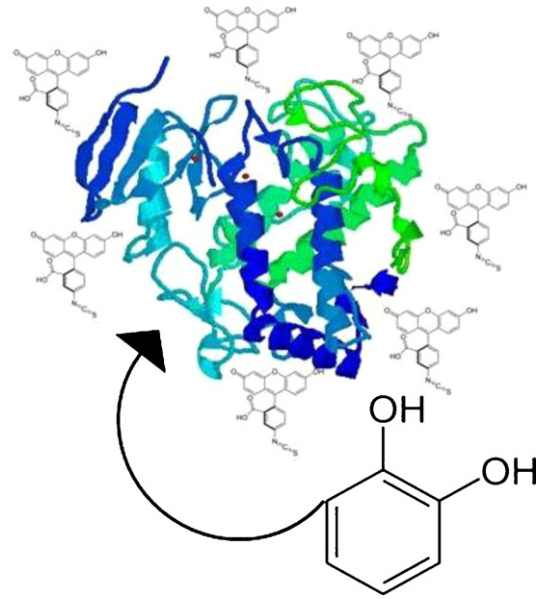

Representative scheme of the catechol-mediated quenching of FITC-labelled tyrosinase. In the presence of catechol, the fluorescence emission of FITC, labelled on the whole enzyme structure, is quenched in a catechol concentration-dependent manner.

Laccase-bisphenol A

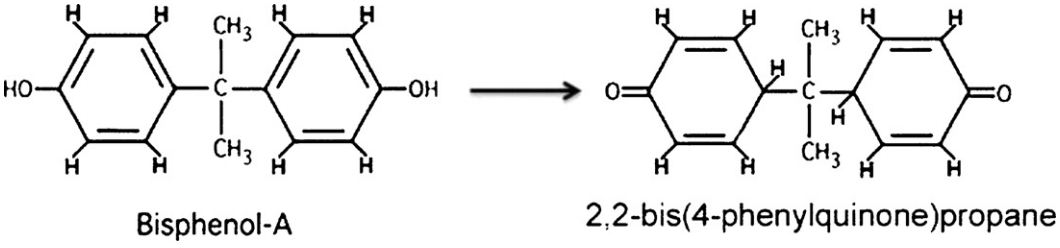

Table 2 (*Continued*)

Hypothetical product of laccase-catalysed oxidation of bisphenol A [26]. The oxidation of bisphenol A brings to a change in the current signals related to the target analyte concentration.	
Chlamydomonas reinhardtii-herbicides	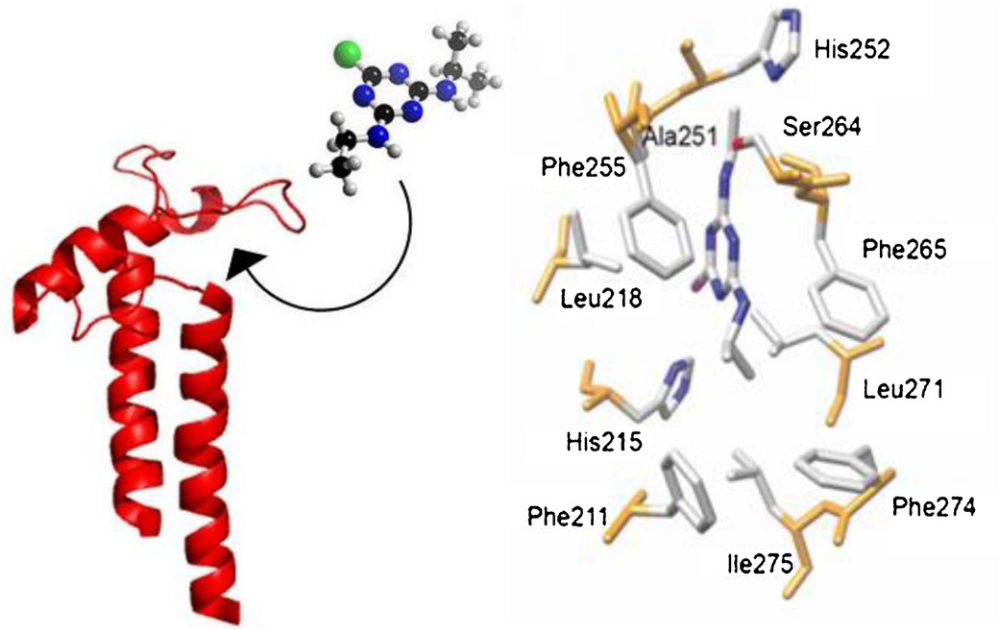
Herbicides target the Q_B binding site of D1 protein, inhibiting the reoxidation of Q_A in PSII. Consequently, the variable fluorescence value $(1 - V_J)$ change in a herbicides concentration-dependent manner. (left) Representative binding of atrazine in the Q_B binding site of D1 protein; (right) molecular details of the atrazine binding site in wild type D1 protein docked complexes [16].	

Legend. AChE: acethylcholinesterase, BChE: butyrylcholinesterase, CNF: carboxynaphthofluorescein, FITC: fluorescein isothiocyanate, LOD: limit of detection, RDS: relative standard deviation.

of 7% and a limit of detection of 50 μM in a linear range between 120 and 500 μM. The regression equation of the linear part of the curve was $y = 3.31 \pm 0.3 \times - 340.24 \pm 25$, where y represents the current in nA and x the catechol concentration in μM; the R^2 was 0.9919. The response time needed to reach 90% of the steady state response was 10 s.

Photosystem II (PSII) from *C. reinhardtii* was utilized in the multipurpose biosensor to reveal photosynthetic herbicides, since it exhibits the ability to recognize certain chemicals in the environment, which produce changes in its physiological activity, such as a variation in the light-induced electron transfer across lipid membranes occurring during the photosynthetic process.

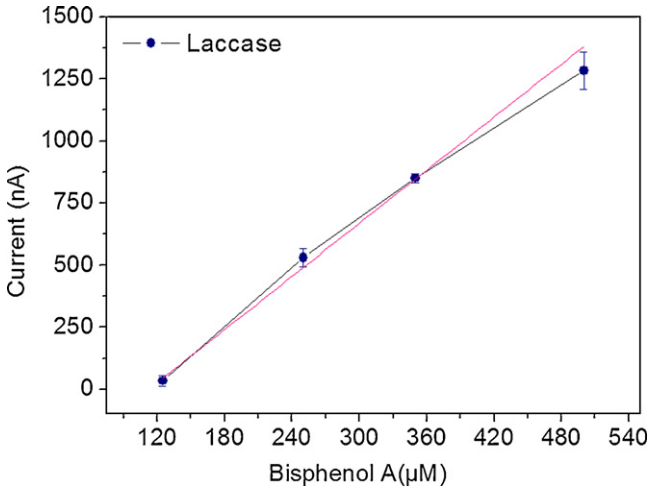

Fig. 7. Calibration curves for bisphenol A by amperometric analysis employing Laccase enzyme.

Under natural in vivo conditions, the photosynthetic system shows a fluorescence behaviour which changes continuously, changing its physiological state and consequently a series of structural and conformational parameters. Pesticides represent an example of chemical species which can influence the shape of the fluorescence transient. These substances are able to target and inhibit Photosystem II at the reducing site, competing with the native plastoquinone at the Q_B-site, with a higher affinity than plastoquinone itself. Consequently, linear electron transport to the cytochrome b6/f-complex is fully or partially blocked. Since the reoxidation of Q_A is inhibited in presence of herbicides, the fluorescence parameters, and in particular the variable fluorescence value $(1 - V_J)$, change in a way that is correlated to herbicides concentration and can be extrapolated from the Kautsky curve [16]. In this paper, we analysed the effect of pesticides belonging to the classes of triazines and ureas, such as atrazine and diuron, classified as EDCs, on the fluorescence parameters of the PSII of *C. reinhardtii*. In particular, we employed a set of mutant strains from the green photosynthetic algae *C. reinhardtii* with different affinity towards these classes of pesticides, in order to obtain unequivocal information about the presence of particular classes and subclasses of pollutants by using a combination of microorganisms. In Fig. 8 the calibration curves for atrazine and diuron were obtained by using three mutant strains from *C. reinhardtii*, which showed limit of detection, towards atrazine and diuron respectively, of 1.6 nM and 0.65 nM for wild-type, 5 nM and 0.48 nM for S268 C strain and 1.9 nM and 0.5 nM for S264 K strain, with an RSD% less than 5%.

The limits of detection of *C. reinhardtii* wild-type and mutant strains were determined on the basis of 99% confidence interval, which, assuming the normal distribution, corresponds to

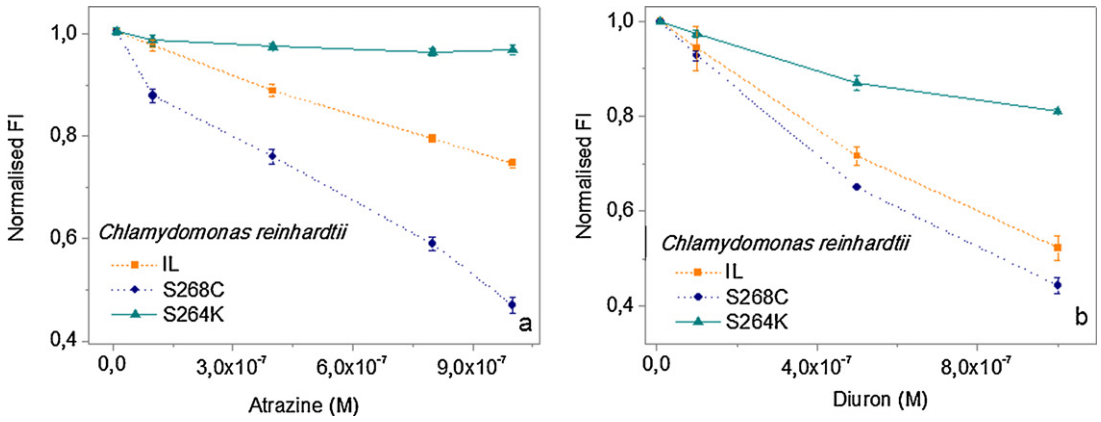

Fig. 8. Calibration curves for atrazine (a) and diuron (b) by optical analysis employing PSII from *C. reinhardtii*.

Table 3
Analytical quality parameters corresponding to Multitask biosensor and laboratory set-up analysis: linear correlation coefficients (r^2), working range (w.r.), limit of detection (LOD, calculated as 3 time of standard deviation of blank/slope) and relative standard deviation (RSD%, calculated on 5 repetitive measurements of intra- and inter-electrodes analysis and calculated on the slope).

Analytical parameters	Chlorpyrifos		Bisphenol A		Atrazine	
	Multitask	l.s.i.	Multitask	l.s.i.	Multitask	l.s.i.
r^2	0.9941	0.9933	0.9902	0.9965	0.9966	0.9984
w.r. (μM)	10–500	10–500	100–500	100–500	0.01–1	0.01–1
LOD (μM)	4.5	3.8	35	28	0.0016	0.0014
R.S.D. (%)	6	5	7	4	5	4

l.s.i.: laboratory set-up instruments.

2.6 × standard error of the measurement (σ). Using then the modified relationship for the Langmuir absorption isotherm, LOD can be calculated as $\text{LOD} = 2.6 \times \sigma \times I_{50}/(100 - 2.6 \times \sigma)$ as reported by Koblizek [24].

In Table 2 a scheme of the reaction equations and measurement parameters was reported for each biosensor, in order to highlight the complete mechanisms.

The performance of the implemented multi-task biosensor was evaluated against laboratory set-up electrochemical and optical instruments, such as the Bipotentiostat/Galvanostat μSTAT 400 (DropSens s.l. Oviedo, Asturias, Spain) for amperometric analysis and Plant Efficiency Analyzer (PEA, Hansatech Instr. Ltd., Kings Lynn, Norfolk, UK) for fluorescence analysis. Table 3 reported data obtained in order to compare results using the portable Multitask biosensor with the laboratory set-up using electrochemical and optical instruments in terms of sensitivity, reproducibility and linearity.

4. Conclusion

The diagnostics technology may represent an important task for environmental management through the development of analytical methodologies with the best features in terms of sensitivity, response time, automation and integration, portability and low cost [25,26]. The increasing concern of the scientific community and public opinion relative to several environmental pathologies has led to attempts to develop reliable methods able to monitor food, water and soil levels of EDCs, a broad class of contaminants recently recognised as a serious threat toward human health and wildlife. As the world becomes more concerned about the impact that environmental contamination may cause on public health and the ecosystem, the demand for rapid detecting biosensors become a real challenge. Several multi-analyte biosensors have been employed for the detection of pesticides and environmental pollutants, mainly those with EDCs characteristics.

In this context, the application of innovative biosensors for the detection of EDCs may support a competitive environmental protection strategy, based on immobilised biological materials coupled to analytical transduction systems, and integrated into an automated, portable, in-field instrument. This paper focused on the design and the realisation of a multitask biosensor for the detection of several environmental pollutants, well known as endocrine disrupting chemicals. It is based on an array of biocomponents intimately integrated with two transduction systems, to enlarge the range of chemicals that can be monitored at levels relevant for environmental regulation.

Acknowledgments

This work was supported by a grant from MIUR Art. 297, “AGROBIOSENS” project, and by the EU FP7-SME-2008-1 project “BEEP-C-EN” for the benefit of SMEs.

References

[1] T. Hayes, K. Haston, M. Tsui, A. Hoang, C. Haeffele, A. Vonk, Nature 419 (2002) 895–896.
[2] T. Hayes, Bioscience 54 (2004) 1138–1149.
[3] S. Storrs, K.M. Kiesecker, Environ. Health Perspect. 112 (2004) 1054–1057.
[4] J.J.A. Carr, R.R.D. Handy, F.F. Orton, F. Frances, Environ. Toxicol. Chem. 1 (2006) 65–71.
[5] C.R. Propper, Integr. Comp. Biol. 45 (2005) 194–200.
[6] E. Diamanti-Kandarakis, J.P. Bourguignon, L.C. Giudice, R. Hauser, G.S. Prins, A.M. Soto, R.T. Zoeller, A.C. Gore, Endocr. Rev. 30 (2009) 293–342.
[7] S. Harrad, C. Ibarra, M. Robson, L. Melymuk, X. Zhang, M. Diamond, J. Douwes, Chemosphere 76 (2009) 232–238.
[8] P. Nicolopoulou, P. Stamanti, Hum. Reprod. Update 7 (2001) 323–330.
[9] D.M. Schreinemachers, Environ. Health 9 (2010) 1–14.
[10] H. Ochoa-Acuna, J. Frankenberger, L. Hahn, C. Carbajo, Environ. Health Perspect. 117 (2009) 1619–1624.
[11] C.M. Tanner, G.W. Ross, S.A. Jewell, R.A. Hauser, J. Jankovic, S.A. Factor, S.A. Bressman, A. Deligtisch, C. Marras, K.E. Lyons, G.S. Bhudhikanok, D.F. Roucoux, C. Meng, R.D. Abbott, J.W. Langston, Arch. Neurol. 66 (2009) 1106–1113.
[12] C. Washam, Environ. Health Perspect. 114 (2006) 48–49.

[13] R.R. Newbold, E. Padilla-Banks, W.N. Jefferson, J.J. Heindel, Int. J. Androl. 31 (2008) 201–208.
[14] http://ec.europa.eu/environment/endocrine/documents/comm1999_en.htm, (accessed on 21.06.12).
[15] http://ec.europa.eu/environment/endocrine/documents/comm2001_en.htm, (accessed on 21.06.12).
[16] K. Buonasera, G. Pezzotti, V. Scognamiglio, A. Tibuzzi, M.T. Giardi, J. Agric. Food Chem. 58 (2009) 5982–5990.
[17] G. Rea, F. Polticelli, A. Antonacci, V. Scognamiglio, P. Katiyar, S.A. Kulkarni, U. Johanningmeier, M.T. Giardi, Protein Sci. 18 (2009) 2139–2151.
[18] M.T. Giardi, V. Scognamiglio, G. Rea, G. Rodio, A. Antonacci, M. Lambreva, G. Pezzotti, U. Johanningmeier, Biosens. Bioelectron. 25 (2009) 294–300.
[19] V. Scognamiglio, D. Raffi, M. Lambreva, G. Rea, A. Tibuzzi, G. Pezzotti, U. Johanningmeier, M.T. Giardi, Anal. Bioanal. Chem. 394 (2009) 1081–1087.
[20] S. Rodriguez-Mozaz, M.J.L. de Alda, D. Barcelo, Talanta 69 (2006) 377–384.
[21] E. Mauriz, A. Calle, J.J. Manclús, A. Montoya, L.M. Lechuga, Anal. Bioanal. Chem. 387 (2007) 1449–1458.
[22] U. Johanningmeier, M.T. Giardi, Protein Sci. 18 (2009) 2139–2151.
[23] F. Arduini, F. Ricci, C.S. Tuta, D. Moscone, A. Amine, G. Palleschi, Anal. Chim. Acta 580 (2006) 155–162.
[24] M. Koblizek, J. Maly, J. Masojidek, J. Komenda, T. Kucera, M.T. Giardi, A.K. Mattoo, R. Pilloton, Biotechnol. Bioeng. 78 (2002) 110–116.
[25] A. Bolli, P. Galluzzo, P. Ascenzi, G. Del Pozzo, I. Manco, M.T. Vietri, L. Mita, L. Altucci, D.G. Mita, M. Marino, IUBMB Life 60 (2008) 843–852.
[26] V. Scognamiglio, G. Pezzotti, I. Pezzotti, J. Cano, K. Buonasera, D. Giannini, M.T. Giardi, Microchim. Acta 170 (2010) 215–225.